Thin-Walled Structures 123 (2018) 441–451

Contents lists available at ScienceDirect

Thin-Walled Structures

journal homepage: www.elsevier.com/locate/tws

Full length article

Structural deterioration of curved thin-walled structure and recovery by rib installation: Verification with structural optimization algorithm

Yoshiki Fukada[a,*], Haruki Minagawa[b], Chikara Nakazato[b], Takaaki Nagatani[a]

[a] Toyota Motor Corporation, 1200 Mishuku, Susono-shi, Shizuoka-ken 410-1193, Japan
[b] Quint Corporation, 1-14-1 Fuchu-cho, Fuchu, Tokyo 183-0055, Japan

A R T I C L E I N F O

Keywords:
Curved beam
Induced force
Structural optimization
Sectional distortion

A B S T R A C T

Structural improvements for curved-surface thin-walled structures were examined. In such structures, installations of ribs—support structures for out-of-plane deformations—are often effective. These out-of-plane deformations are attributed to internal loadings induced from plane stresses. Shapes of solid curved I-sectional beams models were optimized using a structural optimization algorithm—the traction method. Ribbed structures were created semi-automatically by the structural optimization when adequate rib-triggers—striped shape constraints or humps in the initial shapes—were applied to the models. This result validates the effectiveness of rib installations on curved surface structures. It is notable that the rib formation created substantial topology changes.

1. Introduction

Thin-walled structures often suffer deterioration of structural efficiencies due to out-of-plane deformations, a phenomenon that is especially notable in curved surface structures. Thin-walled curved beams are typical examples of such structures that may have wide ranging applications. There is an extensive body of research examining issues related to curved beams. The first contribution can be seen in the famous textbook by Timoshenko and in papers by the same author [1,2]. Anderson [3] examined practical issues of curved beams both in theory and through experiments, demonstrating various examples of curved beam structures in road vehicles and railway cargoes. Issues related to curved beams have continuously attracted the attention of researchers. Recently, extensive studies in nonlinear regions [5,4], applications of composite materials [6,8,7] and new analysis methodologies [10,9] have been published.

Curved beams lose bending stiffness due to sectional distortions and consequential stress localizations. For example, in I-sectional curved beams, longitudinal bending stresses decrease at the edge of the flanges. As a result, these edge parts carry less load and the bending stiffness is equivalent to that of a narrower beam. Fig. 1 shows a typical example of an I-sectional curved beam. The sectional distortions and the non-uniform stress distributions at the flanges can be seen. Westrup and Silver [11] proposed a concept called the “effective area” to describe these phenomena and derived exact or approximate solutions for several types of curved beams. Schagerl [12] extended this concept to universal curved thin-walled structures. Akita et al. [13] studied curved beams in vessel structures and examined the effects of rib installations that suppress the sectional distortions. Rothwell [14] pointed out the existence of an internal force causing the sectional distortions called “effective lateral pressure” and proposed approximation methods to solve curved beam problems. The formula for this pressure F is as follows:

$$F = \frac{t}{R}\sigma \tag{1}$$

where, σ is the in-plane stress at the mid-plane of the flange, t is the thickness of the flange, and R is the curvature radius of the beam. It should be noted that the work of Westrup and Silver [11] is also based on a similar internal force called “induced radial loadings”. These internal forces may be generalized as follows [15–18]:

$$F = tQ_{lk}\sigma_{lk} \tag{2}$$

where, the given coordinate system is a local coordinate system parallel to the local plane, and Q_{ij} is an inverse of the curvature radius measured along the i and the j directions. Below, this paper calls this internal force the “induced force”.

As Schagerl [12] pointed out, sectional distortions occur due to the induced forces in both curved beams and universal curved thin-walled structures. At a glance, these distortions do not seem to significantly affect structural integrity. However, these parasitic deformations cause additional in-plane strain that change the stress distributions and

* Corresponding author.
E-mail address: yoshiki_fukada@mail.toyota.co.jp (Y. Fukada).

https://doi.org/10.1016/j.tws.2017.10.052
Received 26 April 2017; Received in revised form 11 July 2017; Accepted 31 October 2017
0263-8231/

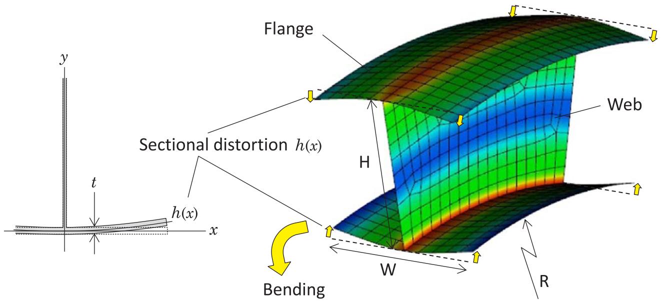

Fig. 1. Curved beam modelled using 2D-shell (the colour contours denote Von-Mises stresses at mid-plane, the loading is constant moment bending, sectional distortions occur at the flanges, and the stress distributions at the flanges are no longer uniform ($H = W = 100$, $R = 500$, $t = 4$).) The $x - y$ plane is set at the section of the beam. (For interpretation of the references to color in this figure legend, the reader is referred to the web version of this article.)

prevent efficient load transfer. It is not easy to identify such weakened parts in actual structures. Li et al. [19] proposed an analysis method to identify these structural weak-points called "micro-lambda λ" and demonstrated an application for an automotive structure. This method described the relationship between the plate stress σ and the plate thickness t as $\sigma \propto t^{-\lambda}$, and regression computations determined the factor λ according to FEA using varying plate thicknesses. According to Li et al., installations of ribs at high λ areas successfully improved the structural efficiency. At those high λ areas, bending of the shell may exist. Some of this bending may be caused by the induced force. An extensive application of this work can be seen in the literature [20].

As pointed out by Anderson [3] and evaluated by Akita et al. [13], installations of ribs are an effective way to recover structural efficiency. Several recently proposed algorithms for structural optimization yield optimum structures based on FEA models [21–26]. These algorithms may be capable of creating appropriate ribs on curved thin-walled structures. However, the automated installation of such ribs has not been implemented.

This study aims to validate this concept—that of induced force and improvement using rib installations— and to implement a trial of automated ribbed structure formation using structural optimization software. There are two categories of structural optimization: topology optimization (i.e., the formation of structures), and shape optimization (i.e., the modification of given structures). This study attempted to apply shape optimization to I-sectional curved beams. This shape optimization is applicable to both shell and solid models. In shell models, formations of new ribs are regarded as changes in topology, which is unattainable using current shape optimization algorithms. Therefore, this study applied the optimization to solid models. As expected, the shape optimization created rib-like structures and the bending stiffness recovered to the level of straight beams. It was also found that adequate triggers are needed. The details are described below.

2. Theory of curved beams

This study only examines the linear region— every displacement is regarded as infinitesimal—, and changes in the moment inertia due to the distortion are not taken into account.

The nominal moment of inertia I_{beam0} can be described as follows:

$$I_{beam0} = I_{flg0} + I_{web} = \frac{t_f WH^2}{2} + \frac{t_w H^3}{12} \tag{3}$$

where, I_{flg0} is the contribution of the flanges and I_{web} is the contribution of the web. The thicknesses of the plates are regarded as sufficiently smaller than the web height H or the flange width W.

As the result of sectional distortion, the longitudinal stresses at the flanges are no longer constant value of (σ_0) but have a distribution $\sigma_L(x)$ as a function of the transverse (along with W) coordinate x. The stress distribution can be described as follows [11,14]:

$$\sigma_L(x) = \sigma_0 - \frac{h(x)}{R}E \tag{4}$$

where, the function $h(x)$ is the displacement of the flange relative to the web —the parasitic sectional distortion—, and E is the Young's modulus of the flanges.

The induced force can be described following Eq. (1):

$$F(x) = \frac{t}{R}\sigma_L(x) \tag{5}$$

The transverse bending of the flanges $h(x)$ can be described as a thin-plate cantilever.

$$\int_x^{\frac{W}{2}} F(\acute{x})(\acute{x} - x)d\acute{x} = \frac{I_{trv}E}{(1-\nu^2)}\frac{d^2 h}{dx^2} \tag{6}$$

where, ν is Poisson's ratio and I_{trv} is the moment of inertia with respect to width for the transverse bending of the flange.

$$I_{trv} = \frac{t^3}{12} \tag{7}$$

These equations can be converted to non-dimensional forms as follows:

$$f(x) \equiv \frac{Eh(x)}{R\sigma_0} \tag{8}$$

$$X \equiv \frac{x}{W} \tag{9}$$

Finally the governing equation is obtained:

$$\int_X^{\frac{1}{2}} (1 - f(\acute{X}))(\acute{X} - X)d\acute{X} = \frac{1}{12(1-\nu^2)}\left(\frac{tR}{W^2}\right)^2 \frac{d^2 f}{dX^2} \tag{10}$$

The parameter tR/W^2 governs the system. Note that Westrup and Silver [11] derived exact solutions for this equation.

The reaction force of the beam is lowered due to the reduced stress $\sigma_L(x)$. This means that the effective moment of inertia I_{flg} decreases from the nominal value I_{flg0}. It can be evaluated as follows:

$$I_{flg} = \frac{\int_0^{W/2} \sigma_L(x)dx}{\int_0^{W/2} \sigma_0 dx} \times I_{flg0} = 2\int_0^{1/2} (1 - f(X))dX \times I_{flg0} \tag{11}$$

Fig. 2 shows the result of Eq. (11). The reduction in the effective moment of inertia is remarkable when tR/W^2 is less than unity. If the transverse bending stiffness of the flanges—I_{trv}—can be sufficiently increased, then the beam bending stiffness may recover. An installation of ribs on the flange as shown in Fig. 3 may be effective because these ribs notably increase the transverse bending stiffness of the flanges even if the ribs are very thin.

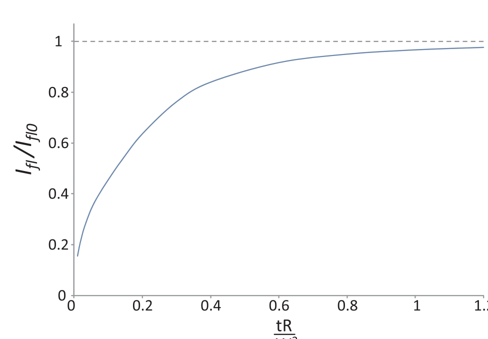

Fig. 2. Effective moment of inertia ($\nu = 0.288$).